Initial Experience with the Radiotracer Anti-1-Amino-3-^{18}F-Fluorocyclobutane-1-Carboxylic Acid with PET/CT in Prostate Carcinoma

David M. Schuster[1], John R. Votaw[1], Peter T. Nieh[2], Weiping Yu[1], Jonathon A. Nye[1], Viraj Master[2], F. DuBois Bowman[3], Muta M. Issa[2], and Mark M. Goodman[1]

[1]Division of Nuclear Medicine, Department of Radiology, Emory University, Atlanta, Georgia; [2]Department of Urology, Emory University, Atlanta, Georgia; and [3]Department of Biostatistics, Emory University, Atlanta, Georgia

Conventional imaging techniques have serious limitations in the detection, staging, and restaging of prostate carcinoma. Anti-1-amino-3-^{18}F-fluorocyclobutane-1-carboxylic acid (anti-^{18}F-FACBC) is a synthetic L-leucine analog that has excellent in vitro uptake within the DU-145 prostate carcinoma cell line and orthotopically implanted prostate tumor in nude rats. There is little renal excretion compared with ^{18}F-FDG. The present study examines anti-^{18}F-FACBC uptake in patients with newly diagnosed and recurrent prostate carcinoma. **Methods:** Fifteen patients with a recent diagnosis of prostate carcinoma (n = 9) or suspected recurrence (n = 6) underwent 65-min dynamic PET/CT of the pelvis after intravenous injection of 300–410 MBq anti-^{18}F-FACBC followed by static body images. Each study was evaluated qualitatively and quantitatively. Maximum standardized uptake values were recorded in the prostate or prostate bed, and within lymph nodes at 4.5 min (early) and 20 min (delayed), and correlated with clinical, imaging and pathologic follow-up. Time–activity curves were also generated for benign and malignant tissue. **Results:** In the 8 patients with newly diagnosed prostate carcinoma who underwent dynamic scanning, visual analysis correctly identified the presence or absence of focal neoplastic involvement in 40 of 48 prostate sextants. Pelvic nodal status correlated with anti-^{18}F-FACBC findings in 7 of 9 patients and was indeterminate in 2 of 9. In all 4 patients in whom there was proven recurrence, visual analysis was successful in identifying disease (1 prostate bed, 3 extraprostatic). In 3 of these patients, ^{111}In-capromab-pendetide had no significant uptake at nodal and skeletal foci. Malignant lymph node uptake in both the staging and restaging patients was significantly higher than benign nodal uptake. Though uptake faded with time, in all 6 patients with either lymph node metastases or recurrent prostate bed carcinoma, there was intense persistent uptake at 65 min. **Conclusion:** Anti-^{18}F-FACBC is a promising radiotracer for imaging prostate carcinoma. Radiotracer uptake was demonstrated in primary and metastatic disease. Future research should investigate the mechanism of radiotracer uptake in normal and pathologic tissue and develop a clinical imaging strategy for initial staging and restaging.

Key Words: anti-^{18}F-FACBC; prostate; neoplasia; PET

J Nucl Med 2007; 48:56–63

Prostate carcinoma is the most common malignancy in men, comprising 33% of newly diagnosed cancers in the United States in 2005 (*1*). Accurately detecting the presence of disease confined to the prostate bed versus that of extraprostatic spread to lymph nodes or the skeletal system has profound treatment implications.

Currently, there is no definitive imaging technique in the initial staging and restaging of prostate carcinoma. Whereas ultrasound and MRI have proven useful for local (T) staging, they have limitations and are not universally used (*2–4*). For local recurrence in the prostate bed, ultrasound-guided transrectal biopsy is often used but it is invasive and subject to sampling error (*5,6*). For lymph node assessment, routine CT and MRI are considered to have poor accuracy (*3,7*).

Molecular imaging techniques such as ^{111}In-capromab pendetide (ProstaScint; Cytogen Corp.) have been used, but sensitivity is only 62%–75% (*3,8,9*). ^{18}F-FDG PET is not of sufficient diagnostic accuracy for routine clinical use for prostate carcinoma (*5,9–14*). Other PET radiotracers, including ^{11}C-acetate, ^{11}C-choline, ^{11}C-methionine, and ^{18}F-fluorocholine (^{18}F-FCH), may characterize different metabolic aspects of prostate carcinoma but have demonstrated mixed results for clinical evaluation (*4,5,10,15–25*). Of course, the ^{11}C-based radiotracers are impractical without an on-site cyclotron. ^{18}F-FCH also seems to have high urinary excretion starting at 5 min after acquisition (*5,19,20,25–28*). Thus, there is a need for a better radiotracer, with little or no urinary excretion, for the evaluation and staging of patients with prostate carcinoma.

Anti-1-amino-3-^{18}F-fluorocyclobutane-1-carboxylic acid (anti-^{18}F-FACBC) is a synthetic L-leucine analog that has excellent in vitro uptake within the DU-145 prostate carcinoma cell line and within orthotopically implanted prostate tumors in nude rats (*29*). The uptake of anti-^{18}F-FACBC is likely mediated via the sodium-independent L large-neutral

Received Jul. 20, 2006; revision accepted Oct. 12, 2006.

For correspondence or reprints contact: David M. Schuster, MD, Department of Radiology, Emory University Hospital, Room E145, 1364 Clifton Rd., Atlanta, GA 30322.

E-mail: david.schuster@emoryhealthcare.org

amino acid transport system (LAT) (*30,31*). There is little renal excretion compared with ^{18}F-FDG (*29*). The present study examines anti-^{18}F-FACBC uptake in patients with newly diagnosed and suspected recurrent prostate carcinoma.

MATERIALS AND METHODS

Preparation of Anti-^{18}F-FACBC

The preparation of anti-^{18}F-FACBC has been previously reported (*32*). The decay-corrected radiochemical yield of the desired product was 24% and its radiochemical purity was 99% at 80 min after the end of bombardment. The injected mass was approximately 5 mg, or 38 μmol, and the specific activity was 136.9–192.4 GBq/mmol (3.7–5.2 Ci/mmol).

Patient Selection

All studies were performed under the auspices of the Emory University Institutional Review Board, Radioactive Drug Research Committee, and the Atlanta Veterans Affairs Medical Center Research and Development Committee. Inclusion criteria included any patient with histologically confirmed prostate carcinoma eligible for prostatectomy and possible lymph node biopsy/dissection or with a prior history of histologically confirmed prostate carcinoma with suspected recurrence or metastatic disease. One patient had been recruited under a prior protocol for imaging renal masses who also happened to have prostate carcinoma. This patient underwent dynamic imaging of the abdomen at the level of the kidneys (otherwise the same protocol as in this study). All newly diagnosed patients were imaged 4–8 wk after the initial prostate biopsy. Prostate-specific antigen (PSA) values were obtained within 4 mo of the anti-^{18}F-FACBC scan. Patient demographics are as follows: mean age ± SD is 62.0 ± 8.8 y with a range of 45–76 y; mean PSA ± SD is 15.0 ± 18.6 ng/mL with a range of 1.9–71 ng/mL; and median Gleason score is 7 with a range of 6–10. The original Gleason scores are used for the patients with suspected recurrence.

PET Imaging Protocol

All scanning was conducted on a Discovery DLS or DST integrated PET/CT scanner (GE Healthcare), and the images were interpreted on a combination of an AW workstation with Volume Viewer Plus (GE Healthcare) as well as a program developed by the authors on the IDL platform (RSI Inc.) running on a Pentium 4 (Intel Corp.) computer (operating system, Microsoft; computer hardware, IBM). All patients fasted for 4–6 h before the anti-^{18}F-FACBC scan. This is our standard practice for ^{18}F-FDG PET, though it has not been established if a fasting or nonfasting state optimizes anti-^{18}F-FACBC imaging. The patient first underwent a CT scan of the abdomen and pelvis (80–120 mA) without oral or intravenous contrast for anatomic correlation and attenuation correction of emission data. The patient then received a bolus of anti-^{18}F-FACBC (300–410 MBq) injected intravenously over 1–2 min. PET consisted of a 15-frame dynamic sequence lasting 65 min (number of frames × time [min]: 6 × 0.5, 4 × 3, and 5 × 10) followed by a static scan of the abdomen and pelvis at 4 min per bed position.

Image Analysis

The PET/CT studies were assessed by 1 experienced nuclear radiologist in a prospective manner. For patients with newly diagnosed prostate carcinoma, the prostate was visually divided into 6 sextants (right and left apex, mid, and base). Three equally spaced regions of interest (ROIs) conforming to the axial dimensions of the sextant were drawn, and the pixel with the greatest standardized uptake value (SUV) in the ROI was noted. The highest of these 3 SUVs was recorded as the maximum SUV (SUV_{max}) for that sextant at the 4.5-min midpoint (3-min frame spanning a dynamic acquisition from 3 to 6 min) and at the 20-min midpoint (10-min frame at 15–25 min). The 4.5-min (early) and 20-min (delayed) frames were chosen based on preliminary analysis of the time–activity curves. In addition, each sextant was visually assessed for the presence of focal activity. A region was considered positive if there was asymmetric focal activity exceeding prostate background activity, similar to the criteria used by Yamaguchi et al. in studying ^{11}C-choline PET (*18*). We augmented visual interpretation by deriving a ratio of sextant SUV_{max} divided by muscle mean SUV (SUV_{mean}) in each patient. The SUV_{mean} was obtained by drawing a 3-cm ROI in each gluteus muscle. SUV_{mean} in muscle was chosen because it remained fairly constant with time and best-simulated typical soft-tissue background. Ideally, we would have chosen a prostatectomy-proven normal sextant as background but this was not possible in most patients.

A lymph node or treated prostate bed was considered visually positive if there was sustained focal activity over expected soft tissue or blood pool. Intensity was recorded as follows: mild (above blood pool but less than muscle), moderate (above muscle but less than marrow), and intense (above marrow). Values of SUV_{max} were also obtained from these lymph nodes or for those of >1 cm in short axis.

Time–Activity Curves

ROIs were defined by hand on transaxial planes over areas of focal uptake or drawn on the CT scan in regions of mild or diffuse uptake. The ROIs included prostate, benign and malignant lymph nodes, bone marrow (ilium), blood pool (femoral artery), muscle (gluteus), bowel (sigmoid), and bladder. Regions of <2 cm in diameter used CT for correction of partial-volume and tissue spillover effects (*33*).

Correlation of Imaging to Clinical Data

Anti-^{18}F-FACBC imaging findings were correlated with pathologic, clinical, biochemical, and imaging follow-up for up to 1 y after scanning. For local disease, this included pathologic analysis of prostatectomy as well as prostate biopsy tissue. A lymph node was considered clinically positive if there was pathologic proof of neoplasia or progressive increase in lymph node size in the presence of elevated PSA. The absence of lymph node involvement was confirmed if there was a negative surgical lymph node dissection or biopsy or, if lymph node dissection was not performed, PSA declining to nadir (<0.05) after definitive therapy, or if there were no enlarged lymph nodes on follow-up imaging at 6 mo. If a pelvic lymph node dissection was not performed and the patient was placed on hormonal therapy, lymph node status was considered indeterminate.

Statistical Analysis

Nonparametric statistical methods were applied for analyses, given the limited sample size in our study. We assessed all between-group differences in SUV_{max} using the Wilcoxon rank sum test. Statistical significance was determined using a type-I error rate of $\alpha = 0.05$, and specific P values are reported with the results. The statistical analyses were performed using SAS version 9.1 software. Statistical significance was reported only if $n > 2$ in each comparison group.

TABLE 1
Anti-^{18}F-FACBC Pathologic Malignant vs. Benign Sextant SUV_{max} and SUV_{max}/Muscle SUV_{mean} Ratios at Early (4.5 Minutes) and Delayed (20 Minutes) Time Points for Initial Staging of Patients

Patient	Time point	Malignant SUV_{max}	Benign SUV_{max}	Malignant sextant/muscle ratio	Benign sextant/muscle ratio
1	Early	7, 9.4, 5.6, 9.3, 9.2, 3.8		9.1, 12.2, 7.3, 12.1, 11.9, 4.9	
	Late	4.8, 5.1, 3.9, 5.9, 5.3, 3.6		4.5, 4.8, 3.7, 5.6, 5.0, 3.4	
2	Early	7.4, 7.6, 11.2, 7.4, 7.7, 8.1		11.9, 12.3, 18.1, 11.9, 12.4, 13.1	
	Late	4.3, 4.9, 4.8, 4.3, 4.5, 4.3		4.5, 5.1, 5.0, 4.5, 4.7, 4.5	
3	Early	6.8, 6.5, 5.8, 6.9, 5.6	5.1	14.5, 13.8, 12.3, 14.7, 11.9	10.9
	Late	5.7, 5.4, 5.2, 5.5, 4.3	4.6	7.6, 7.2, 6.9, 7.3, 5.7	6.1
4	Early	2.2, 2.5, 1.6, 2.1, 2.0, 1.8		4.4, 5.0, 3.2, 4.2, 4.0, 3.6	
	Late	2.8, 2.8, 1.9, 2.4, 2.2, 1.7		4.0, 4.0, 2.7, 3.4, 3.1, 2.4	
5	Early	4.5, 5.8, 4.4	3.6, 4.6, 3.3	4.1, 5.3, 4.0	3.3, 4.2, 2.8
	Late	6.0, 5.3, 5.0	3.2, 3.2, 3.0	3.8, 3.4, 3.2	2.0, 2.3, 1.8
6	Early	6.7, 6.7, 4.1	5.8, 5.5, 4.6	6.8, 6.8, 4.1	5.9, 5.6, 4.6
	Late	5.6, 4.3, 3.0	3.4, 3.5, 3.2	3.9, 3.0, 2.1	2.4, 2.5, 2.3
7	Early	6.5, 8.9, 5.5, 5.0, 8.2, 6.6		13.5, 18.5, 11.5, 10.4, 17.1, 13.8	
	Late	5.0, 4.7, 3.9, 5.0, 5.7, 4.7		6.8, 6.4, 5.3, 6.8, 7.7, 6.4	
8	Early	6.6, 6.3, 4.4, 4.5	4.5, 4.8	6.5, 6.2, 4.3, 3.5	4.4, 4.7
	Late	4.3, 4.2, 4.3, 4.4	4.1, 3.9	3.0, 2.9, 3.0, 2.4	2.8, 2.7
n (mean ± SD)		39	9	39	9
	Early	6.0 ± 2.3*	4.6 ± 0.8*	9.4 ± 4.6†	5.2 ± 2.3†
	Late	4.4 ± 1.1‡	3.6 ± 0.5‡	4.6 ± 1.6§	2.8 ± 1.3§

*$P = 0.05$.
†$P = 0.01$.
‡$P = 0.01$.
§$P = 0.0005$.

RESULTS

Initial Staging

Eight patients underwent dynamic prostate imaging and were correlated with either sextant biopsy ($n = 4$) or histologic examination of the surgically removed prostate ($n = 4$). Thirty-nine sextants were positive for carcinoma (1 with a minute focus) and 9 were negative (1 with chronic inflammation). Visual analysis predicted the presence or absence of carcinoma in 40 of 48 sextants. Table 1 is a listing of sextant values of SUV_{max} and ratios of SUV_{max} to muscle SUV_{mean} for each patient. A typical patient example is presented in Figure 1.

In correlation of lymph node status, 7 of 9 patients had excellent concordance of anti-^{18}F-FACBC pelvic nodal findings with clinical follow-up. Two of 9 were indeterminate. Table 2 is a summary of lymph node concordance and Figure 2 is an example of a patient with lymph node metastases. Both patients with malignant lymph nodes had intense persistent uptake, even at 65 min, though less intense than on earlier sequences.

The representative time–activity curve taken from patient 3 (Fig. 3) shows rapid uptake of anti-^{18}F-FACBC in prostate carcinoma to a maximum at 4.5 min, followed by gradual clearance (9.5%/min) beyond 20 min. Regions in marrow (ilium), muscle (gluteus), and bladder reached a plateau at 4.5 min, which remained constant throughout the imaging period. This activity time course was consistent across the patient population for malignant prostate and normal tissues.

Suspected Recurrence

On a per-patient basis, the anti-^{18}F-FACBC scan detected neoplasia in 4 of 4 patients with proven recurrence. In 3 of

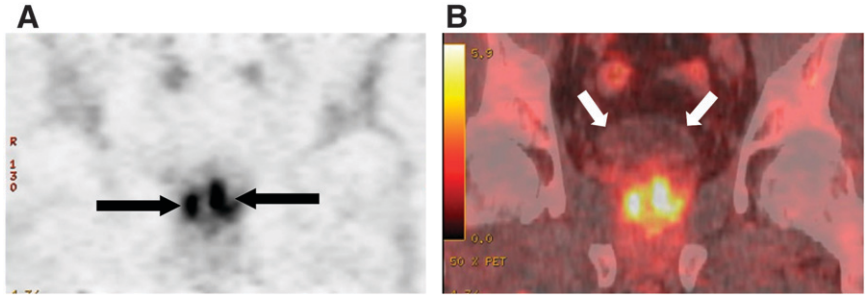

FIGURE 1. Coronal PET (A) and CT fused (B) anti-^{18}F-FACBC images of 63-y-old male patient with pathologically proven bilateral prostate carcinoma (arrows in A). Note little bladder activity (white arrows in B).

TABLE 2
Abdominal/Pelvic Lymph Node Imaging Findings for Initial Staging of Patients at Early (4.5 Minutes) and Delayed (20 Minutes) Time Points with Clinical/Pathologic Correlation

Patient	PSA (ng/mL)	GS	Anti-^{18}F-FACBC imaging visual uptake: early; late SUV_{max}	Clinical/pathologic correlation	Comments
1	8.4	7	No uptake	Indeterminate	PLND 11 mo after anti-^{18}F-FACBC scan, 1 node positive
2	71	9	Intense: 11.7 ± 3.2; 4.4 ± 1.3 (n = 5)	Malignant nodes	PSA rising to 290 ng/mL and enlarging pelvic nodes on serial CT scans
3	11	7	No uptake	No malignant nodes	Negative PLND
4	21	8	No uptake	Indeterminate	Not surgical candidate, systemic therapy
5	6.3	9	Moderate fading to mild uptake: 3.7 ± 0.1, 3.2 ± 0.0 (n = 2)	No malignant nodes	Negative PLND; uptake in benign-appearing inguinal nodes
6	16.2	6	No uptake	No malignant nodes	PSA nadir (<0.05) after cryotherapy
7	5.7	6	No uptake	No malignant nodes	No PLND; negative follow-up abdomen/pelvic CT at 6 mo
8	5.7	8	No uptake	No malignant nodes	Negative PLND
9	2.7	10	Intense: 8.3 ± 0.8, 8.4 ± 11.1 (n = 3)	Malignant nodes	Positive biopsy, extensive retroperitoneal nodes
Mean ± SD	Malignant		10.5 ± 3.0 (early); 5.9 ± 2.4 (late) (n = 8)	7/9 concordance	
	Benign		3.7 ± 0.1 (early); 3.2 ± 0.0 (late) (n = 2)		

GS = maximum Gleason score; PLND = pelvic lymph node dissection.

these patents, ^{111}In-capromab-pendetide was unrevealing. In 2 of 6 patients, mild-to-moderate uptake in the prostate bed resulted in false-positive scans, presumably from the radiation effect noted on biopsy. These 2 patients also had negative anti-^{18}F-FACBC and conventional imaging of extraprostatic sites. A summary of each patient's case is presented in Table 3.

There was intense, easily identifiable uptake in the one recurrent prostate bed (Fig. 4) and in the 3 patients with nodal/skeletal metastases (Fig. 5). Uptake in the 2 false-positive prostate beds was less intense and less focal than that in the 1 true recurrent site. Mild diffuse uptake below blood-pool background was present in the other treated beds. Similar to the initial staging of patients, intense uptake persisted on the 65-min images in all 3 patients with lymph node/skeletal metastases and in the 1 patient with recurrent prostate bed carcinoma (though less intense than on the earlier sequences).

The representative time–activity curve taken from restaging patient 1 (Fig. 6A) shows rapid uptake of anti-^{18}F-FACBC in known prostate carcinoma recurrence to a maximum at 4.5 min with a plateau to 30 min, which is followed by gradual clearance (9%/min) out to 60 min. Regions in marrow (ilium), muscle (gluteus), and bladder reached a plateau at 4.5 min that remained constant throughout the imaging period.

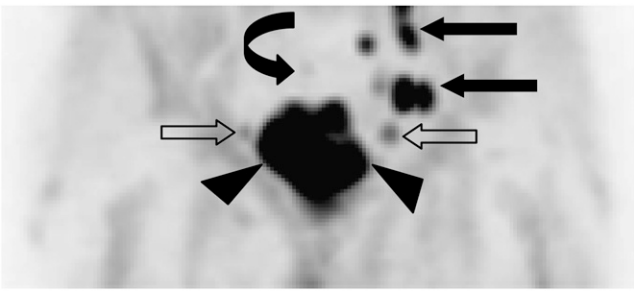

FIGURE 2. A 73-y-old man with extensive invasive prostate carcinoma, with bilateral obturator and left iliac chain lymph nodal involvement. Maximum-intensity-projection image demonstrates extent of large prostate primary (arrowheads) as well as bilateral obturator (open arrows) and left iliac (solid straight arrows) nodes. Bladder activity is not present (curved arrow at bladder location).

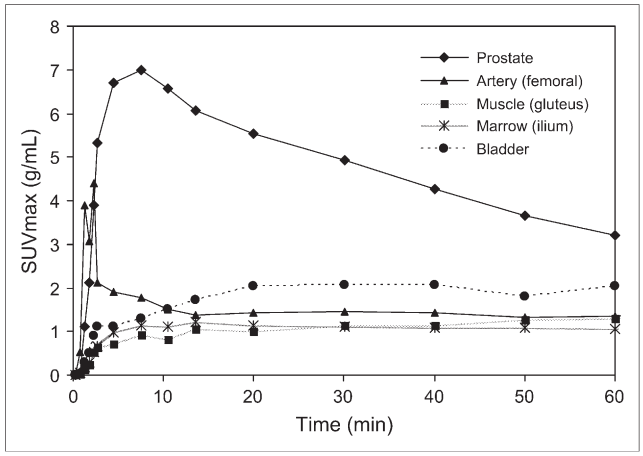

FIGURE 3. Time–activity curves for initial staging data. Time–activity curve compares uptake in whole prostate with known bilateral carcinoma vs. bladder, marrow, muscle, and femoral artery in initial staging of patient 3.

TABLE 3
Imaging Findings for Suspected Recurrence in Prostate Beds and in Lymph Nodes at Early (4.5 Minutes) and Delayed (20 Minutes) Time Points with Clinical/Pathologic Correlation

Patient	History	PSA (ng/mL)	Anti-^{18}F-FACBC uptake: early; late SUV_{max}		Presence of carcinoma	Comments
			Prostate bed	Lymph nodes		
1	Subtotal prostatectomy	43.5	Focal intense: 5.8; 6.4	No uptake	Bed: positive; LN: indeterminate	Positive biopsy bed; no other follow-up
2	Brachytherapy, XRT, salvage cryotherapy	11.7	Focal moderate seminal vesicle: 4.1; 3.0	Intense: 9.6 ± 6.1; 6.3 ± 4.5 (n = 2)	Bed: indeterminate; LN: positive	No biopsy bed; PSA rising and enlarging nodes on serial CT scans
3	Brachytherapy	4.1	Diffuse mild uptake: 3.9; 2.7	Intense: 5.7; 5.3 (n = 1)*	Bed: negative; LN: positive	Radiation-effect bed; positive laparoscopic LN sampling*
4	Brachytherapy, XRT	1.9	Focal mild–moderate: 4.1; 3.8	No uptake	Bed: negative; LN: indeterminate	Radiation effect bed†
5	Brachytherapy	6.8	Linear moderate central: 4.6; 3.9	No uptake‡	Bed: negative; LN: indeterminate	Radiation effect bed†‡
6	Prostatectomy, salvage radiotherapy	9.5	Diffuse mild uptake: 2.8; 2.7	Intense: 10.5 ± 4.0; 12.3 ± 5.0 (n = 3)	Bed: indeterminate; LN: positive	Positive sternal biopsy, nodes enlarging on CT and PSA rising; prostate bed not biopsied§
Mean ± SD	Malignant		5.8 (early); 6.4 (late) (n = 1)	9.4 ± 4.2 (early); 9.1 ± 5.1 (late)‖ (n = 6)	4/4 concordance (3 had negative ^{111}In-capromab-pendetide)	
Clinically or pathologically proven	Benign		4.2 ± 0.4 (early); 3.5 ± 0.7 (late) (n = 3)	2.8 ± 0.8 (early); 1.4 ± 0.3 (late)‖ (n = 4)		

*Patient 3 also had moderate fading to mild uptake in benign-appearing inguinal node (SUV_{max} = 3.7 early, 1.8 late) and biopsy-proven benign obturator nodal grouping (SUV_{max} = 3.3 early, 1.5 late).
†Patients 4 and 5 had subsequently decreasing PSA. Postbrachytherapy prolonged PSA bump is clinically suggested but more follow-up is needed.
‡Patient 5 had moderate fading to mild uptake in 2 benign-appearing inguinal nodes (SUV_{max} = 2.2 and 2 early, 1.1 and 1.2 late).
§Patient 6 had skeletal metastases that were also intensely positive on anti-^{18}F-FACBC scan.
‖P = 0.01 on early and delayed images.
LN = lymph nodes.

The time–activity curve for patient 3 (Fig. 6B) compares uptake in a malignant right internal iliac lymph node with benign right inguinal and obturator nodes. The clearance of the benign regions is more abrupt between 4.5 and 10 min (30%/min) and then slows to that of the malignant region.

DISCUSSION

On the basis of in vitro and in vivo studies (*29,34,35*), we hypothesized that anti-^{18}F-FACBC would be able to serve as a valuable adjunct in the initial staging of prostate carcinoma, as well as detecting the presence of local versus

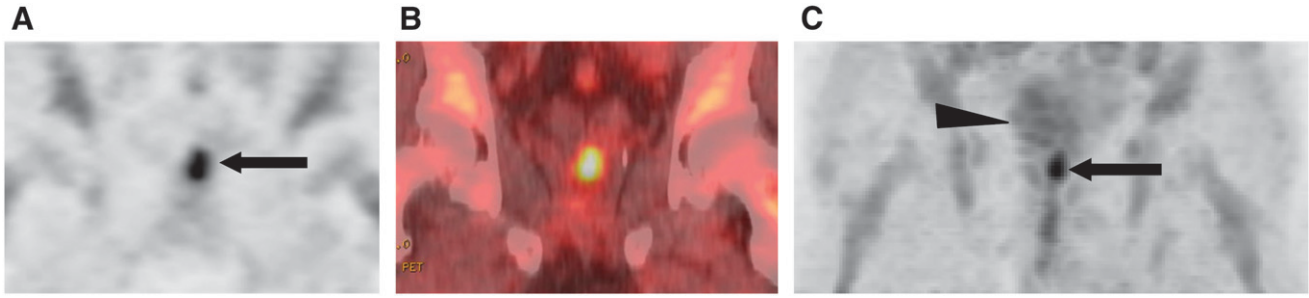

FIGURE 4. Coronal PET (A) and CT fused (B) anti-^{18}F-FACBC images in 71-y-old male patient (restaging patient 1) with biopsy-proven prostate bed recurrence extending toward left seminal vesicle (arrow in A). Maximum-intensity-projection image at 20 min (C) demonstrates uptake in prostate bed (arrow) but little bladder uptake (arrowhead).

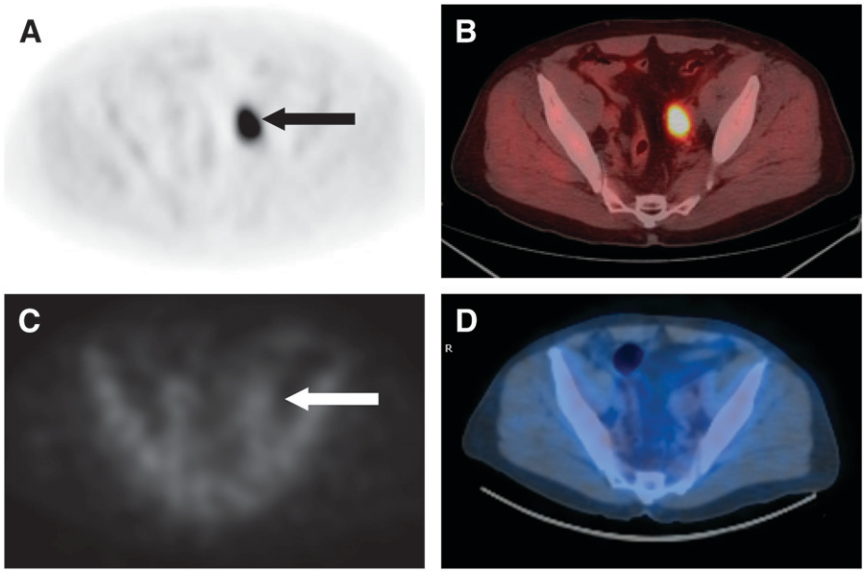

FIGURE 5. Axial PET (A) and fused (B) anti-^{18}F-FACBC images in 67-y-old male patient (restaging patient 2) with intense activity in left external iliac nodes (black arrow in A). SPECT/CT ^{111}In-capromab-pendetide axial ^{111}In (C) and CT fused (D) images demonstrate no significant activity in this region (white arrow in C).

metastatic prostate carcinoma in the setting of biochemically recurrent disease. The present study demonstrates encouraging but preliminary initial results.

Anti-^{18}F-FACBC seems to share characteristics with other PET radiotracers used for prostate scanning. Similar to ^{11}C-acetate and ^{18}F-FCH (*4,20,36*), we observed a certain degree of nonspecific uptake, including relatively intense incidental bowel uptake as well as occasional low-level uptake in benign inguinal lymph nodes.

We also noted regions of false positivity and negativity within the prostate. Though malignant sextants had statistically significant higher SUV_{max} than benign sextants, there was little separation between benign and malignant sextant values of SUV_{max}. Yet, visual analysis revealed that there was agreement of 40 of 48 sextants with pathologic results, and ratios of sextant uptake to mean muscle SUV_{max} demonstrated improved, though still incomplete, separation of malignant from benign tissue. Some pathologically identified benign prostate tissue, including that with inflammation, had focal uptake but these were visually less intense than malignant disease. Future studies will be designed to better examine the question of uptake in inflammatory versus neoplastic foci within the same prostate.

Uptake within the prostate in areas of inflammation, hyperplasia, and high-grade prostatic intraepithelial neoplasia has also been reported with ^{18}F-FCH, ^{11}C-choline, and ^{11}C-acetate (*4,5,21,24,37*). Kwee et al. (*25*) noted better discrimination between malignant and benign prostatic regions using early and 1-h delayed prostate imaging with ^{18}F-FCH. It remains to be seen whether anti-^{18}F-FACBC imaging may be useful for primary tumors and to separate areas of inflammation and hyperplasia from neoplasia.

Anti-^{18}F-FACBC demonstrates potential clinical benefit for nodal staging. Formal lymph node dissection is a highly morbid procedure, and anti-^{18}F-FACBC may prove valuable in directing biopsy. For both staging and restaging, SUV_{max} of malignant nodes was significantly higher than that of benign nodes and anti-^{18}F-FACBC helped discriminate prostatic from extraprostatic involvement. It is also interesting to note that 3 patients with negative ^{111}In-capromab-pendetide studies had positive anti-^{18}F-FACBC imaging, proven to be true positive.

Choline-based compounds have also shown similar promise in nodal staging and in detecting recurrence (*4,15*). Although intense bladder activity has been reported 5 min after injection with ^{18}F-FCH (*5,19,26*), anti-^{18}F-FACBC demonstrates relatively little, though variable, renal excretion and bladder activity. Even the most intense bladder activity did not interfere with scan interpretation as has been reported with choline-based PET radiotracers. Yet, the mechanism of anti-^{18}F-FACBC uptake in prostate carcinoma cells is not well understood and is the basis of ongoing studies. Preliminary data suggest a major role for an LAT transporter (*30,31*).

The time–activity curves of Figures 3 and 6 show rapid uptake of anti-^{18}F-FACBC to 4.5 min, which is followed quickly by a fast and then slow washout rate out to 60 min. Tracer retention in background structures for all cases approaches a plateau after the first 4.5 min. More detailed analysis of the uptake mechanisms awaits further study, but metabolite analysis of arterial plasma samples in human subjects indicates that anti-^{18}F-FACBC does not undergo metabolism (Mark M. Goodman, unpublished data, July 2006).

These findings also suggest that anti-^{18}F-FACBC may be less useful for delayed imaging in some patients because of washout of radiotracer. Yet, all 6 patients with either locally recurrent prostate carcinoma or lymph node metastases did have persistent and often striking uptake, even at 1 h, which may reflect increased uptake in neoplastic cells prone to metastasize or recur. More comprehensive studies must be undertaken to further determine the significance of these findings, to define the optimal time course of imaging, and

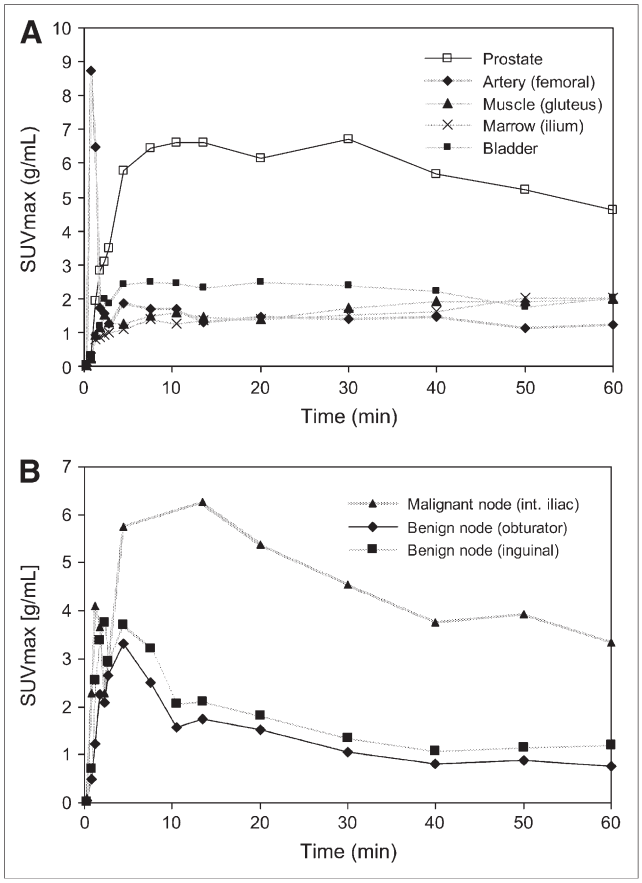

FIGURE 6. Time–activity curve for restaging patient 1 (A) compares uptake in known prostate bed carcinoma recurrence vs. bladder, marrow, muscle, and femoral artery. Time–activity curve in restaging patient 3 (B) compares uptake in a 14 × 11 mm right internal iliac malignant node with benign right inguinal 12 × 18 mm node and benign right obturator 7 × 18 mm conglomerate.

to find out if comparing early to delayed imaging could increase specificity.

One shortcoming of our study is that step-section pathology was not obtained, and some cases only had sextant biopsy for correlation. There may be a discrepancy between what is perceived as a certain sextant on transrectal ultrasonography biopsy and sextant pathologic analysis after prostatectomy (*38*). Another shortcoming was our methodology using SUV_{max}. We chose SUV_{max} because this is the most common clinical method of SUV use. However, it is less suitable when evaluating regions with low uptake. We attempted to overcome this limitation by applying a ratio of SUV_{max} to muscle SUV_{mean}, which more closely approximated results with visual interpretation. Future studies will be designed to incorporate more sophisticated tools, such as 3-dimensional mapping, as well as correlation with step-section pathology.

This study is a pilot investigation with a small and heterogeneous patient population. Tests for statistical significance, therefore, were based on a limited sample size. Because of clinical exigencies, not all patients underwent prostatectomy and lymph node dissection, and not all lymph nodes were biopsied. All benign causes of uptake, including that from inflammation, were grouped together, and a definitive subanalysis of benign inflammatory versus noninflammatory uptake was not possible.

CONCLUSION

Imaging with anti-^{18}F-FACBC demonstrated uptake in both primary and metastatic prostate carcinoma on initial staging as well as uptake in recurrent prostate carcinoma within the prostate bed, lymph nodes, and bone. Anti-^{18}F-FACBC PET/CT succeeded in identifying neoplastic foci, even when ^{111}In-capromab-pendetide was negative, and was instrumental in directing biopsy to prove neoplastic recurrence in one patient in whom lymph nodes were not obviously enlarged. Thus, it is feasible that anti-^{18}F-FACBC could improve diagnostic imaging of prostate carcinoma both before and after therapy. A larger cohort study will be designed to establish the clinical utility of anti-^{18}F-FACBC PET/CT in primary and suspected recurrent prostate carcinoma.

ACKNOWLEDGMENTS

This research was sponsored by Nihon Medi-Physics Co., Ltd. We acknowledge the hard work of Fenton G. Ingram, CNMT, on this protocol as well as all of our technologists at Emory HealthCare and the patients who volunteered for the study. We also gratefully acknowledge the contributions of Ron Crowe for radiotracer synthesis, Drs. Adam Kuehn and Mahul B. Amin for histologic interpretation, Dr. Raghuveer K. Halkar for imaging consultation, and Dr. Fray F. Marshall for clinical urologic guidance.

REFERENCES

1. Jemal A, Murray T, Ward E, et al. Cancer statistics, 2005. *CA Cancer J Clin.* 2005;55:10–30.
2. Scardino P. Update: NCCN prostate cancer clinical practice guidelines. *J Natl Compr Canc Netw.* 2005;3 (*suppl 1*):S29–S33.
3. Brassell SA, Rosner IL, McLeod DG. Update on magnetic resonance imaging, ProstaScint, and novel imaging in prostate cancer. *Curr Opin Urol.* 2005;15: 163–166.
4. Schmid DT, John H, Zweifel R, et al. Fluorocholine PET/CT in patients with prostate cancer: initial experience. *Radiology.* 2005;235:623–628.
5. Schoder H, Larson SM. Positron emission tomography for prostate, bladder, and renal cancer. *Semin Nucl Med.* 2004;34:274–292.
6. Fowler JE Jr, Brooks J, Pandey P, Seaver LE. Variable histology of anastomotic biopsies with detectable prostate specific antigen after radical prostatectomy. *J Urol.* 1995;153:1011–1014.
7. Sartor O, McLeod D. Indium-111-capromab pendetide scans: an important test relevant to clinical decision making. *Urology.* 2001;57:399–401.
8. Lange PH. ProstaScint scan for staging prostate cancer. *Urology.* 2001;57:402–406.
9. Seltzer MA, Barbaric Z, Belldegrun A, et al. Comparison of helical computerized tomography, positron emission tomography and monoclonal antibody scans for evaluation of lymph node metastases in patients with prostate specific antigen relapse after treatment for localized prostate cancer. *J Urol.* 1999;162: 1322–1328.
10. Dimitrakopoulou-Strauss A, Strauss LG. PET imaging of prostate cancer with ^{11}C-acetate. *J Nucl Med.* 2003;44:556–558.

11. Shreve PD, Grossman HB, Gross MD, Wahl RL. Metastatic prostate cancer: initial findings of PET with 2-deoxy-2-[F-18]fluoro-D-glucose. *Radiology.* 1996; 199:751–756.
12. Schoder H, Herrmann K, Gonen M, et al. 2-[^{18}F]Fluoro-2-deoxyglucose positron emission tomography for the detection of disease in patients with prostate-specific antigen relapse after radical prostatectomy. *Clin Cancer Res.* 2005;11: 4761–4769.
13. Larson SM, Morris M, Gunther I, et al. Tumor localization of 16β-^{18}F-fluoro-5α-dihydrotestosterone versus ^{18}F-FDG in patients with progressive, metastatic prostate cancer. *J Nucl Med.* 2004;45:366–373.
14. Hofer C, Laubenbacher C, Block T, Breul J, Hartung R, Schwaiger M. Fluorine-18-fluorodeoxyglucose positron emission tomography is useless for the detection of local recurrence after radical prostatectomy. *Eur Urol.* 1999;36:31–35.
15. de Jong IJ, Pruim J, Elsinga PH, Vaalburg W, Mensink HJ. Preoperative staging of pelvic lymph nodes in prostate cancer by ^{11}C-choline PET. *J Nucl Med.* 2003;44:331–335.
16. Toth G, Lengyel Z, Balkay L, Salah MA, Tron L, Toth C. Detection of prostate cancer with ^{11}C-methionine positron emission tomography. *J Urol.* 2005;173: 66–69.
17. Kwee SA, Coel MN, Lim J, Ko JP. Prostate cancer localization with ^{18}fluorine fluorocholine positron emission tomography. *J Urol.* 2005;173:252–255.
18. Yamaguchi T, Lee J, Uemura H, et al. Prostate cancer: a comparative study of ^{11}C-choline PET and MR imaging combined with proton MR spectroscopy. *Eur J Nucl Med Mol Imaging.* 2005;32:742–748.
19. DeGrado TR, Coleman RE, Wang S, et al. Synthesis and evaluation of ^{18}F-labeled choline as an oncologic tracer for positron emission tomography: initial findings in prostate cancer. *Cancer Res.* 2001;61:110–117.
20. Price DT, Coleman RE, Liao RP, Robertson CN, Polascik TJ, DeGrado TR. Comparison of [^{18}F]fluorocholine and [^{18}F]fluorodeoxyglucose for positron emission tomography of androgen dependent and androgen independent prostate cancer. *J Urol.* 2002;168:273–280.
21. Yoshida S, Nakagomi K, Goto S, Futatsubashi M, Torizuka T. ^{11}C-Choline positron emission tomography in prostate cancer: primary staging and recurrent site staging. *Urol Int.* 2005;74:214–220.
22. Fricke E, Machtens S, Hofmann M, et al. Positron emission tomography with ^{11}C-acetate and ^{18}F-FDG in prostate cancer patients. *Eur J Nucl Med Mol Imaging.* 2003;30:607–611.
23. Oyama N, Akino H, Kanamaru H, et al. ^{11}C-Acetate PET imaging of prostate cancer. *J Nucl Med.* 2002;43:181–186.
24. Farsad M, Schiavina R, Castellucci P, et al. Detection and localization of prostate cancer: correlation of ^{11}C-choline PET/CT with histopathologic step-section analysis. *J Nucl Med.* 2005;46:1642–1649.
25. Kwee SA, Wei H, Sesterhenn I, Yun D, Coel MN. Localization of primary prostate cancer with dual-phase ^{18}F-fluorocholine PET. *J Nucl Med.* 2006;47:262–269.
26. Hara T, Kosaka N, Kishi H. Development of ^{18}F-fluoroethylcholine for cancer imaging with PET: synthesis, biochemistry, and prostate cancer imaging. *J Nucl Med.* 2002;43:187–199.
27. Heinisch M, Dirisamer A, Loidl W, et al. Positron emission tomography/computed tomography with F-18-fluorocholine for restaging of prostate cancer patients: meaningful at PSA
28. de Jong IJ, Pruim J, Elsinga PH, Vaalburg W, Mensink HJ. ^{11}C-Choline positron emission tomography for the evaluation after treatment of localized prostate cancer. *Eur Urol.* 2003;44:32–38.
29. Oka S, Hattori R, Kurosaki F, et al. A preliminary study of anti-1-amino-3-^{18}F-fluorocyclobutyl-1-carboxylic acid for the detection of prostate cancer. *J Nucl Med.* 2007;48:46–55.
30. Martarello L, McConathy J, Camp VM, et al. Synthesis of syn- and anti-1-amino-3-[^{18}F]fluoromethyl-cyclobutane-1-carboxylic acid (FMACBC), potential PET ligands for tumor detection. *J Med Chem.* 2002;45:2250–2259.
31. McConathy J, Martarello L, Simpson NE, et al. Uptake profiles of six ^{18}F-labeled amino acids for tumor imaging: comparison of in vitro and in vivo uptake of branched chain and cyclobutyl amino acids by 9L gliosarcoma tumor cells. *J Nucl Med.* 2002;43 (*suppl*):41P.
32. McConathy J, Voll RJ, Yu W, Crowe RJ, Goodman MM. Improved synthesis of anti-[^{18}F]FACBC: improved preparation of labeling precursor and automated radiosynthesis. *Appl Radiat Isot.* 2003;58:657–666.
33. Kessler RM, Ellis JR Jr, Eden M. Analysis of emission tomographic scan data: limitations imposed by resolution and background. *J Comput Assist Tomogr.* 1984;8:514–522.
34. Oka S, Hattori R, Kurosaki F, et al. Biodistribution and microPET imaging of anti-[^{18}F]FACBC using orthotopic prostate tumor transplantation model in rats. *J Nucl Med.* 2005;46 (*suppl*):381P.
35. Schuster DM, Votaw JR, Nieh PT, et al. Initial experience with the radiotracer anti 1 amino 3 [^{18}F]fluorocyclobutane-1-carboxylic acid (anti-[^{18}F]FACBC) with PET/CT in newly diagnosed prostate cancer. *J Nucl Med.* 2006;47 (*suppl*):224P.
36. Oyama N, Miller TR, Dehdashti F, et al. ^{11}C-Acetate PET imaging of prostate cancer: detection of recurrent disease at PSA relapse. *J Nucl Med.* 2003;44:549–555.
37. Kato T, Tsukamoto E, Kuge Y, et al. Accumulation of [^{11}C]acetate in normal prostate and benign prostatic hyperplasia: comparison with prostate cancer. *Eur J Nucl Med Mol Imaging.* 2002;29:1492–1495.
38. Wefer AE, Hricak H, Vigneron DB, et al. Sextant localization of prostate cancer: comparison of sextant biopsy, magnetic resonance imaging and magnetic resonance spectroscopic imaging with step section histology. *J Urol.* 2000;164:400–404.